

The Protein Composition of the Digestive Fluid from the Venus Flytrap Sheds Light on Prey Digestion Mechanisms*[§]

Waltraud X. Schulze[‡], Kristian W. Sanggaard[§], Ines Kreuzer[¶], Anders D. Knudsen[§], Felix Bemm^{||}, Ida B. Thøgersen[§], Andrea Bräutigam^{‡‡}, Line R. Thomsen[§], Simon Schliesky^{‡‡}, Thomas F. Dyrland[§], Maria Escalante-Perez[¶], Dirk Becker[¶], Jörg Schultz^{||}, Henrik Karring^{§§}, Andreas Weber^{‡‡}, Peter Højrup^{¶¶}, Rainer Hedrich^{¶¶¶¶**}, and Jan J. Enghild^{§**}

The Venus flytrap (*Dionaea muscipula*) is one of the most well-known carnivorous plants because of its unique ability to capture small animals, usually insects or spiders, through a unique snap-trapping mechanism. The animals are subsequently killed and digested so that the plants can assimilate nutrients, as they grow in mineral-deficient soils. We deep sequenced the cDNA from *Dionaea* traps to obtain transcript libraries, which were used in the mass spectrometry-based identification of the proteins secreted during digestion. The identified proteins consisted of peroxidases, nucleases, phosphatases, phospholipases, a glucanase, chitinases, and proteolytic enzymes, including four cysteine proteases, two aspartic proteases, and a serine carboxypeptidase. The majority of the most abundant proteins were categorized as pathogenesis-related proteins, suggesting that the plant's digestive system evolved from defense-related processes. This in-depth characterization of a highly specialized secreted fluid from a carnivorous plant provides new information about the plant's prey digestion mechanism and the evolutionary processes driving its defense pathways and nutrient acquisition. *Molecular & Cellular Proteomics* 11: 10.1074/mcp.M112.021006, 1306–1319, 2012.

From the [‡]Max Planck Institut für Molekulare Pflanzenphysiologie, Am Mühlenberg 1, 14476 Potsdam, Germany; [§]Department of Molecular Biology and Genetics, Aarhus University, Gustav Wiedsvej 10C, 8000 Aarhus C, Denmark; [¶]Department of Molecular Plant Physiology & Biophysics, Universität Würzburg, Julius-von-Sachs-Platz 2, 97082 Würzburg, Germany; ^{||}Department of Bioinformatics, Biozentrum, Am Hubland, Universität Würzburg, D-97074 Würzburg, Germany; ^{‡‡}Department of Plant Biochemistry, Heinrich-Heine-Universität Duesseldorf, Universitaetsstrasse 1, 40225 Duesseldorf, Germany; ^{§§}University of Southern Denmark, Institute of Chemical Engineering, Biotechnology and Environmental Technology, Niels Bohrs Allé 1, 5230 Odense M, Denmark; ^{¶¶}Department of Biochemistry and Molecular Biology, University of Southern Denmark, Campusvej 55, 5230 Odense M, Denmark; ^{|||}Zoology Department, College of Science, King Saud University, P.O. Box 2455, Riyadh 11451, Saudi Arabia

Received June 5, 2012, and in revised form, July 26, 2012

Published, MCP Papers in Press, August 12, 2012, DOI 10.1074/mcp.M112.021006

Carnivorous plants capture, digest, and “eat” animals using four different types of trapping strategies: (i) flypaper or adhesive traps (e.g. *Drosera*, also known as sundews, and *Pinguicula*, also known as butterworts), (ii) sucking bladder traps (e.g. *Utricularia*, also known as bladderworts), (iii) pitfall traps (e.g. *Nepenthes*), and (iv) snap traps (e.g. *Dionaea muscipula*, also known as the Venus flytrap). These plants fascinated Charles Darwin. The Venus flytrap, in particular, attracted his attention, and he described the plant as “one of the most wonderful in the world” (1). The snap trap most likely evolved from the adhesive trap, because its ability to capture larger prey than the adhesive traps gives it an evolutionary advantage (2).

The trapping motion of *Dionaea muscipula* is among the fastest movements in the plant kingdom, and its mechanism has been described in detail, starting with Charles Darwin's work from ~150 years ago (3–6). The plant's leaves employ turgor pressure and hydrodynamic flow to close the trap (3). The closing is initiated by the mechanical stimulation of trigger hairs, eliciting an action potential to close the trap, which seals the fate of the animal inside (1). Then “touch” hormones such as 12-oxophytodienoic acid, which is a precursor of the phytohormone jasmonic acid, probably induce the secretion of digestive fluid (7). Touch hormones are likely to be released in response to the continuous mechanical stimulation of the trigger hairs by the prey as it struggles to escape (7). The trap may also be closed artificially by direct electrical stimulation or by the application of the bacterial phytotoxine coronatine (5, 7, 8).

The largest classes of Venus flytrap prey are spiders and flies. Highly active fliers, such as bees and wasps, are rarely caught (9). The trapped animal faces a slow death, and experiments with ants demonstrate that the prey are alive and capable of stimulating the trigger hairs up to 8 h after being caught (10). The nutrients obtained from the digestion of the different prey are important for the Venus flytrap. Among carnivorous plants in their natural habitats, the Venus flytrap appears to be the most dependent on the nitrogen obtained

from its digested prey (11). The nutrients from insects and spiders give the plants a competitive advantage in their natural low-nutrient soil habitats (12).

In contrast to its trapping mechanism, only a few studies have focused on the digestion process of the Venus flytrap, and none of the involved enzymes has been purified. However, the pH during Venus flytrap digestion has been studied. The pH of the digestive fluid is 4.3, and during the secretion phase the external “stomach” is further acidified to pH 3.4 (7, 13). The optimum pH for protease activity in the fluid has been analyzed in different studies, and the resulting values range from pH 3.0 to pH 7.0 (13–16). This discrepancy is likely due to differences in the assay conditions and the substrates used as targets during the analyses (13, 16).

In our work, we have determined the protein composition of the digestive fluid of the Venus flytrap. The protein identifications were based on a two-step approach involving (i) deep sequencing of the cDNA from stimulated leaves (RNA-seq) and (ii) subsequent mass spectrometric (MS)¹ analyses of the proteins in the collected digestive fluids (Fig. 1). Both the RNA-seq analyses and the digestion fluid proteomics were performed on independent samples using complementary approaches. The obtained mass spectra were searched against the two generated transcriptome databases, and the identified proteins in the secretome were abundance-ranked based on their intensity sums. Our results provide insights into the complex composition of the Venus flytrap’s digestive fluid, which has vital functions in defense and nutrient digestion.

EXPERIMENTAL PROCEDURES

Plant Material for 454 Sequencing and Sampling by Filter Paper Stimulation—*Dionaea muscipula* plants were purchased from CRESCO Carnivora (De Kwakel, The Netherlands) and grown in plastic pots at 22 °C in a 16:8 h light:dark photoperiod. Three stimulation methods were used for the transcriptomic approach: (i) the plants were fed with ants, and the traps were collected after 24 h; (ii) the plants were sprayed with 100 μM coronatine, and the traps were harvested after 24 h; and (iii) the plants were stimulated by the placement of filter paper soaked with either 30 mM urea, 30 mM chitin, or water into the trap, and trap tissue was collected 1 and 8 h after stimulation. The material for the transcriptome analyses was harvested as follows: traps and excised trigger hairs were frozen in liquid nitrogen. Additionally, secretory cells were isolated from the inner trap surface by gently abrading the gland complexes using a razor blade. RNA was separately isolated from each sample, and for cDNA synthesis, the RNA from different tissues was pooled.

To stimulate fluid secretion for the protein analyses, the closure of healthy mature traps was initiated by tickling the trigger hairs within the trap. Because secretion does not begin without further stimulation of the trigger hairs while the trap is in the closed state, a fine piece of filter paper soaked with water was trapped in the closing snap trap, allowing for the induced movement of the trigger hairs by slight movements of the filter paper. Secreted liquid was then carefully sampled from the closed trap using a pipette tip that was inserted between the closed trap lobes.

¹ The abbreviations used are: DTT, dithiothreitol; LC, liquid chromatography; MS, mass spectrometric.

Plant Material for Illumina Sequencing and Sampling by Magnet-based Stimulation—Plants were purchased at the Lammehave nursery (Ringe, Denmark) and grown in a walk-in plant growth chamber at 26 °C in a 12:12 h light:dark photoperiod. All of the experiments were performed on healthy mature plants. For the transcriptomics analyses, the digestion process was initiated by feeding the plants yellow mealworm beetles (*Tenebrio molitor*). After 3, 8, 24, 48, and 72 h, the leaves were harvested, rinsed with water to remove the partially digested beetle and beetle fragments, snap frozen in liquid nitrogen, and stored at –80 °C. For each time point, two stimulated traps were harvested.

For the protein analyses, magnet-based stimulation of the leaf was used to induce the secretion of the digestive fluid. A small stick-magnet was positioned between the trap leaves, and 100 μl of the cysteine protease inhibitor trans-epoxysuccinyl-l-leucylamido-(4-guanidino) butane (E-64; 50 μM) was added to the trap to reduce the level of adventitious proteolysis (14, 16). Then a larger magnet was applied to move the smaller magnet inside the trap, stimulating the trigger hairs and resulting in complete closure. After 48 and/or 72 h, the secreted fluid (up to 200 μl) was aspirated using a pipette that was forced in between the leaf lobes of the trap. The collected material was centrifuged, and the supernatant was used for further analyses. If not used immediately, the fluid was stored at –20 °C.

Transcriptome Sequencing and Assembly—The leaves from the stimulated traps were pooled and homogenized before RNA was extracted using a previously described hot borate buffer protocol (17). Poly-A transcripts were enriched from 3.5 μg of total RNA, and the transcripts were fractionated in the presence of Zn²⁺. Subsequently, double-stranded cDNA synthesis was performed using random primers and RNase H. After end repair and purification, the fragments were ligated with bar-coded paired-end adapters, and fragments with insert sizes of ~150 to 250 bp were isolated from an agarose gel. Half of the library was normalized, and the other half was amplified via PCR and purified from a gel. The library quality was assessed using capillary sequencing of randomly selected clones. The high-throughput sequencing of the cDNA samples from the beetle-stimulated traps was performed on an Illumina HiSeq 2000 instrument using a paired-end run with 2 × 50 bp. The cDNA samples isolated from the traps from the other combined stimulation approach were sequenced using a 454 GS FLX Titanium platform. The filtered reads from the two transcriptomic datasets were assembled using Oases software (56) on top of Velvet and Mira, respectively. The minimum size for the assembly was set to either 50 or 100 bases. Several parameter sets (e.g. Burrows-Wheeler Alignment) were tested to optimize the assemblies.

Sampling Procedures for Proteomics—For the filter paper stimulation method, the secreted fluid was collected into three independent pools from 15 to 20 traps stimulated for 68 h. The protein was precipitated using ice-cold acetone. Protein pellets were resuspended in 6 M urea and 2 M thiourea (pH 8). After the reduction of disulfide bonds with dithiothreitol (DTT), free cysteine residues were alkylated using iodoacetamide. Proteins were predigested with Lys-C for 3 h before the dilution of the sample with four volumes of 10 mM Tris-HCl (pH 8). Trypsin was added (1 μg trypsin per 50 μg protein), and the digestions were performed at room temperature for 16 h. After acidification, the peptides were desalted over a C18 matrix prior to the MS analysis.

For the magnet-based method, digestive fluid was collected 48 h after the stimulation of 18 traps. Subsequently, three pools were prepared using the digestive fluid from five to eight plants. From these samples, 35 μl were withdrawn, and the pH was adjusted to 8.5. Subsequently, DTT was added, the samples were boiled for 5 min, and iodoacetamide was then added to alkylate free cysteine residues. After 15 min of incubation, trypsin was added (1:20 ratio), and the digestions were performed at 37 °C for 16 h.

Gel-free Proteomics of the Digestive Fluid (from Both Sampling Procedures)—The resulting peptides from each of the digests were separated using an EasyLC nanoflow HPLC system (Proxeon Biosystems, Odense, Denmark) connected to an LTQ-Orbitrap XL mass spectrometer (Thermo Fisher Scientific) equipped with a nanoESI ion source (Proxeon Biosystems, Odense, Denmark). The chromatographic separation was performed on a 15-cm fused silica emitter (100 μm i.d.) that was in-house packed with RP ReproSil-Pur C18-AQ 3 μm resin (Dr. Marisch GmbH, Ammerbuch-Entringen, Germany). The peptides were eluted using an acidic acetonitrile gradient at a flow rate of 250 nl min^{-1} , as described elsewhere (18, 19).

MS scans (300–1800 m/z) were recorded using an Orbitrap mass analyzer at a resolution of 60,000 at 400 m/z , with 1×10^6 automatic gain control target ions and a 500-ms maximum ion injection time. The MS scans were followed by data-dependent collision-induced dissociation MS/MS scans of the five most intense multiply charged ions in the mass spectrometer at a 15,000 signal threshold, 30,000 automatic gain control target, 300-ms maximum ion injection time, 2.5- m/z isolation width, 30-ms activation time at 35 normalized collision energy, and dynamic exclusion enabled for 30 s with a repeat count of 1. Peak picking was performed using either MaxQuant 1.114 (Max Planck Institute of Biochemistry, Martinsried, Germany) or Xcalibur 2.0 (Thermo Fisher Scientific Inc., Waltham, MA). The raw data files of the in-solution digestion of the Venus flytrap secretion fluid from both sampling methods have been deposited at the Tranche database (proteomecommons.org) under the following hash key: `tzwFTnv4Y04ujdmGC1tVaULYKS3OQ/0i3pmQ2P0vvvdHe6+5vX09E6zW4OzKILOJJDZ9OTXzOB8N66+5czMOCv2MORA-AAAAAAAAE/A=.`

Identification and Quantification of the Secretome Proteins Using the 454 Transcriptome—The acquired raw data files were searched against the 6-frame translation of the 454 transcriptome (in total, 227,604 protein entries) using MaxQuant 1.114 (20). The carbamidomethylation of cysteine residues was set as a fixed modification, and the oxidation of methionine residues was set as a variable modification. Two missed cleavages were allowed. The mass tolerance for the first search was set to 10 ppm, and the fragment mass tolerance was set to 0.5 Da. The peptide and protein false discovery rates were set to 0.01, and the identified peptides were required to have a minimum length of six amino acid residues. The assignment of the identified peptides to translated proteins was primarily based on proteotypic peptides. Peptides with more than one protein match were assigned to protein groups consisting of all of the proteins with their respective peptide matches. The retention time alignment of the precursor ions was used to extract intensity information from the peaks with matching m/z values from samples in which these peaks were not selected for data-dependent fragmentation.

Identification and Quantification of the Secretome Proteins Using the Illumina Transcriptome—For protein identification, the raw data from both sampling procedures were searched against the 6-frame translation of the Illumina transcriptome (in total, 97,728 protein entries) using Mascot 2.3.02 (Matrix Science, London, UK) (21). The searches were performed with up to one missed cleavage allowed, carbamidomethyl (C) as a fixed modification, methionine oxidation as a variable modification, a peptide mass tolerance offset of 10 ppm, a fragment mass tolerance of 0.5 Dalton, and an ion score cutoff at 20. Peptide identification was defined as peptides with scores above Mascot's homology threshold and at a significance threshold (p) of 0.01. Peptide assignments to proteins were performed according to the default Mascot settings, *i.e.* each redundant peptide was primarily assigned to the highest scoring protein. The described settings resulted in an average false discovery rate of 3.3%. However, additional stringent criteria for protein and peptide acceptances were applied (see below). Proteins that did not meet the quantitative thresholds and

that were not identified and quantified in at least two of the six samples were rejected. To extract the quantitative information, Mascot Distiller 2.4.2.0 (Matrix science) was applied using fraction and correlation thresholds of 0.7 and 0.9, respectively. The data were parsed using MS Data Miner 1.0, which is in-house-developed software (57).

Gel-based Proteomics of the Digestive Fluid—A total of 100 μl of digestive fluid from the magnet-stimulated traps was lyophilized and subsequently dissolved in SDS sample buffer containing 30 mM DTT. The proteins were resolved in 5% to 15% acrylamide gradient gels (23). Subsequently, the gel was silver-stained, and all of the visible bands were excised and digested with trypsin (24, 25). Tryptic peptides were purified using a C18 stage tip (Proxeon Biosystem A/S part of Thermo Fisher Scientific Inc., Odense, Denmark) and were subsequently analyzed via liquid chromatography (LC)-MS/MS using an EASY-nLC (Proxeon Biosystems) connected to a Q-TOF Ultima API (Micromass/Waters, Milford, MA) mass spectrometer. As described above, the obtained mass spectra were analyzed using Mascot; however, the significant threshold value (p value) was set at 0.05 because of the lower complexity of the samples and the lower sensitivity of the instrument. In addition, the peptide mass tolerance was set at 1 Dalton because of the lower accuracy of this instrument. If the identification was based on a single peptide, then it was accepted only if the protein was also observed during the gel-free analyses using the more sensitive Orbitrap mass spectrometers.

Verification of the Peptide and Protein Assignments—We manually verified that the peptide hits corresponding to the same transcript corresponded to the same reading frame. If the peptides were identified from different reading frames, then we evaluated whether the different reading frames were likely explained by missing regions in the sequence of interest, which could have led to a frameshift. If this was the case, then the reading frames that resulted in the identification of peptides were merged in the part of the transcript that was missing (see “X” in the sequences). If the identification was based on one unique peptide, then the MS/MS data were manually validated using the following criteria: the assignment of major peaks and the occurrence of uninterrupted γ - or β -ion series of at least three amino acid residues. The full list of identified peptides and proteins can be found in [supplemental Tables S1](#) (454 transcriptome) and [S2](#) (Illumina transcriptome). The spectra for proteins with single-peptide identifications can be found in [supplemental Figs. S2](#) (454 transcriptome, in-solution analysis), [S3](#) (Illumina transcriptome, in-solution analysis), and [S4](#) (Illumina transcriptome, gel analysis). The majority of the proteins were identified and quantified by means of both the Mascot/Illumina transcriptome approach and the MaxQuant/454 transcriptome approach, which strengthens our data.

Determination of the Proteins' Relative Abundances—To calculate the relative abundances, we initially calculated the sum of the ion intensities from the extracted ion chromatograms for all of the identified peptides in that particular analysis (*i.e.* the total ion intensity). Subsequently, the individual samples were normalized. Then, the relative abundance (or fraction of the total) of a particular protein (weighted by the protein's molecular weight) was derived using the following formula: (MS intensity sum for the peptides belonging to a specific protein/total ion intensity of the sample)/molecular weight of the transcript. Subsequently, the average value of the relative abundances was calculated based on samples from the same stimulation method when the protein was present. The abundance ranking performed here was similar to the emPAI calculation (26); however, we based our rankings on summed ion intensities rather than peptide counts, which is analogous to the iBAQ quantification (27). Transcript molecular weight was used for protein size normalization. If only one or two peptides were identified and quantifiable for a single protein, then those peptides were used for quantitation in any case. Proteins

TABLE I
Transcriptome properties

	Illumina	454
Number of contigs	16,288	37,934
Sum of the contig lengths	12,177,595	21,138,288
Cut-off contig length	100	50
Average length of the contigs	747	550

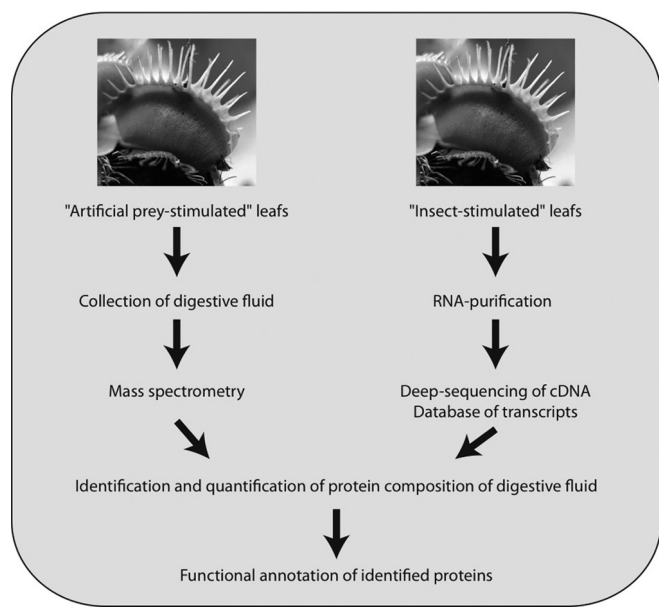


FIG. 1. Workflow of the Venus flytrap digestive fluid analysis.

were excluded if they were identified and quantifiable in only one of the six LC-MS/MS samples. We focused on the identified proteases in the Results section, and we searched specifically for proteases in the obtained data. Consequently, if the identified protein was a protease, then we carefully searched the peptide spectra, and if acceptable (see supplemental Fig. S2) the protein was included in Table II even if it was identified and quantified in only one of the six samples. Based on this screening, only contig 18374 was included.

Functional Annotation and Alignment Analyses—Each identified protein was functionally annotated via comparison with *Arabidopsis thaliana* using the TAIR BLAST 2.2.8 tool with the default settings (www.arabidopsis.org). The highest scoring hit was used for the annotation. If a homologous protein was not identified using this approach, a comparison with the NCBI nr database was performed using the NCBI BLAST tool. The MEROPS peptidase database (merops.sanger.ac.uk) and the Biology Workbench software from the San Diego Supercomputer Center (workbench.sdsc.edu) were used for sequence analyses and alignments of the identified proteolytic enzymes (28).

RESULTS

Deep Sequencing of the cDNA from Stimulated Venus Flytrap Snap Trap Leaf Lobes—In the present study, we used transcriptomics-generated databases to facilitate the subsequent proteomics-based identification and quantification of the proteins in Venus flytrap digestive fluid (Fig. 1). To increase the likelihood of including all of the relevant transcripts, we employed two different deep sequencing RNA-seq technologies to generate two comprehensive cDNA databases. After the raw data were cleaned, the 454 transcriptome was assembled from 3.5 million reads. In total, 37,934 contigs with matching homologies in the plant kingdom were assembled with an average length of 550 (Table I). In the Illumina transcriptome, ~41 and 120 million paired-end reads of 50 bp lengths were obtained for the non-normalized sample and the normalized sample, respectively. The data from these two

sequencing runs were combined and used for contig and transcript assemblies. A hash value of 41 was selected for the contig and transcript assembly, and 16,288 transcripts were assembled with an average length of 747 (Table I).

The Basic Pattern of the Protein Composition of the Venus Flytrap Digestive Fluid—If the Venus flytrap plants had been stimulated to secrete digestive fluid by a natural prey, then the peptides derived from “prey proteins” would have influenced the mass spectrometry analyses, likely affecting the sensitivity of the analyses, as well as the quantification and identification of the secreted Venus flytrap proteins. A standardized protocol for digestive fluid harvesting would have been difficult to implement if natural prey had been used. Instead, we developed two methods to stimulate the secretion of the digestive fluid without adding real prey.

Upon magnet-based stimulation, the secretion process was initially monitored over 3 days. After 24 h, moisture was detected in the traps, but the amounts were too small for sampling. Up to 200 μ l of digestive fluid was collected 48 h (10 replicates) and 72 h (three replicates) after stimulation. The traps that were emptied after 48 h were allowed to continue to secrete for an additional 24 h after stimulation (three replicates). The proteins in the collected samples were separated by SDS-PAGE (supplemental Fig. S1), resulting in the same pattern of protein bands. This suggested that the variation over time and from plant to plant in the overall protein composition of the digestive fluid was low under the conditions employed.

Identification and Abundance Ranking of the Proteins in the Venus Flytrap Digestive Fluid—The secreted proteins from the magnet-based and filter-paper-based stimulations were analyzed by LC-MS/MS. Six datasets were searched against both of the generated transcriptomes and analyzed using MaxQuant and Mascot Distiller. Using this approach, we identified and quantified 76 proteins in the digestive fluid (Table II, supplemental Table S3), with 32 proteins detected in both transcripts. Furthermore, 34 were present in only the 454 transcriptome (supplemental Tables S1 and S4), and 10 proteins were present in only the Illumina transcriptome (supplemental Tables S2 and S5). In total, 66 proteins were identified in the secreted fluid upon filter-paper-based stimulation, and 42 proteins were identified in the secretion fluid after magnet-based stimulation (Table II). Of these 42 proteins, 30 proteins were also identified upon filter-paper-based stimulation, demonstrating large overlap (71%) between the sampling proce-

The Composition of the Digestive Fluid of the Venus Flytrap

TABLE II
List of the identified and quantified proteins from the secreted fluid after two different stimulation methods (paper-based and magnet-based) and after matching against two different transcriptomes (454 and Illumina); the abundance ranking within each sample is indicated

Identifier (454-transcript)	Identifier (Illumina-transcript)	Accession (A. thaliana)	Putative function	Average rank in both transcripts	
				Paper-based stimulation	Magnet-based stimulation
	Locus_8322_Transcript_1/ 1_Confidence_1.000		No BLAST hit with E-value < 1	5	1
DM_TRA02_REP_contig53074	Locus_610_Transcript_2/ 2_Confidence_1.000	AT3G12500	Chitinase	5	2
NG-5590_Gland_cleanedcontig148924	Locus_223_Transcript_110/ 117_Confidence_0.063	AT5G45890	Cysteine protease (dionain-3)	6	3
DM_TRA02_REP_contig82037	Locus_223_Transcript_111/ 117_Confidence_0.063	AT4G33720	No BLAST hit with E-value < 1	16	4
DM_TRA02_REP_contig53027	Locus_369_Transcript_1/ 1_Confidence_1.000	AT4G33355	PR (pathogenesis-related) protein	5	5
DM_TRA02_contig15221	Locus_270_Transcript_1/ 2_Confidence_1.000	AT4G11650	PR (pathogenesis-related) protein	20	5
DM_TRA02_REP_contig50549	Locus_270_Transcript_1/ 2_Confidence_1.000	AT4G11650	Osmotin-like protein	29	6
DM_TRA02_contig105872	Locus_326_Transcript_1/ 1_Confidence_1.000	AT1G11905	Protein of unknown function	22	6
DM_TRA02_REP_contig53296	Locus_1885_Transcript_2/ 2_Confidence_1.000	AT4G33355	PR (pathogenesis-related) protein	54	7
NG-5590_Gland_cleanedcontig74818& contig124417	Locus_21_Transcript_5/ 6_Confidence_0.188	AT5G45890; AT1G	Cysteine protease (dionain-2)	10	9
NG-5590_Gland_cleanedcontig110078	Locus_326_Transcript_1/ 1_Confidence_1.000	AT1G47128	Cysteine proteinase (Dionain 4)	24	10
DM_TRA02_contig14398	Locus_1885_Transcript_2/ 2_Confidence_1.000	AT2G38530	Lipid transfer protein	8	11
DM_TRA02_contig352	Locus_2155_Transcript_2/ 2_Confidence_1.000	AT5G06860	Polygalacturonase inhibiting protein	13	11
NG-5590_Gland_cleanedcontig146186	Locus_3837_Transcript_1/ 1_Confidence_1.000	AT3G10410	Serine carboxypeptidase-like 49	15	13
DM_TRA02_contig19199	Locus_673_Transcript_1/ 1_Confidence_1.000	AT2G02990	Ribonuclease T2 family	1	14
DM_TRA02_contig16330	Locus_52_Transcript_2/ 5_Confidence_0.385	AT3G57260	Beta 1,3-glucanase	2	15
NG-5590_Gland_cleanedcontig2880	Locus_448_Transcript_1/ 1_Confidence_1.000	AT1G14540	Peroxidase superfamily protein	20	15
DM_TRA02_contig33225	Locus_3455_Transcript_1/ 1_Confidence_1.000	AT5G54370	Late embryogenesis abundant protein	20	16
DM_TRA02_REP_contig51333	Locus_462_Transcript_4/ 6_Confidence_0.200	AT5G59970	No BLAST hit with E-value < 1	20	17
DM_TRA02_contig18767	Locus_522_Transcript_1/ 2_Confidence_1.000	AT4G35790	Histone superfamily protein	25	17
DM_TRA02_REP_contig85615	Locus_522_Transcript_1/ 2_Confidence_1.000	AT1G53130	Protein with phospholipase D activity	25	18
DM_TRA02_REP_contig55271	Locus_21_Transcript_3/ 6_Confidence_0.562	AT1G51060	PR (pathogenesis-related) protein	25	18
DM_TRA02_contig14593	Locus_462_Transcript_2/ 6_Confidence_0.300	AT5G45890	A histone H2A protein	27	19
	Locus_5180_Transcript_1/ 1_Confidence_1.000	XP_002510033 AT4G26880	Cysteine proteinase (dionain-1)	27	19
		AT1G79820	Branched Chain amino acid pathway Stigma-specific Stig1 family protein	27	20
			Suppressor of G protein beta1 (SGB1)	27	21

TABLE II—continued

Identifier (454-transcript)	Identifier (Illumina-transcript)	Accession (A. thaliana)	Putative function	Average rank in both transcripts	
				Paper-based stimulation	Magnet-based stimulation
DM_TRA02_contig12450	Locus_5610_Transcript_1/ 1_Confidence_1.000	AT5G05340	Peroxidase superfamily protein	19	22
DM_TRA02_REP_contig78697	Locus_6940_Transcript_1/ 1_Confidence_1.000	AT5G05340	No BLAST hit with E-value < 1 Peroxidase superfamily protein	15	22
DM_TRA02_contig53&contig6292	Locus_8046_Transcript_1/ 1_Confidence_1.000	AT5G05400	Purple acid phosphatase 27 (PAP27)	21	22
DM_TRA02_contig14693	Locus_5274_Transcript_1/ 2_Confidence_0.800	AT2G07698	No BLAST hit with E-value < 1 ATPase, F1 complex, alpha subunit protein	10	23
NG-5590_Gland_cleanedcontig104489	Locus_597_Transcript_3/ 3_Confidence_0.667	AT4G35790	Encodes a protein with phospholipase D activity	32	24
DM_TRA02_contig7401	Locus_597_Transcript_3/ 3_Confidence_0.667	AT5G14780	NAD-dependent formate dehydrogenase	33	25
DM_TRA02_contig16324	Locus_864_Transcript_1/ 1_Confidence_1.000	AT3G04720	PR (pathogenesis-related) protein	41	26
DM_TRA02_contig24716	Locus_5734_Transcript_1/ 1_Confidence_1.000	AT5G06860	No BLAST hit with E-value < 1 Polygalacturonase inhibiting protein	18	27
DM_TRA02_REP_contig50397	Locus_5734_Transcript_1/ 1_Confidence_1.000	AT2G27130	Lipid transfer protein (LTP) family protein precursor	5	28
DM_TRA02_contig9524	Locus_187_Transcript_30/ 39_Confidence_0.191	AT4G26880	Lysm domain GPI-anchored protein 2	35	28
DM_TRA02_REP_contig63924	Locus_9868_Transcript_1/ 1_Confidence_1.000	AT5G45960	stigma-specific Stig1 family protein	41	30
DM_TRA02_contig6244	Locus_5819_Transcript_1/ 1_Confidence_1.000	AT4G39330	Cinnamyl alcohol dehydrogenase 9	4	31
DM_TRA02_REP_contig53347	Locus_2276_Transcript_1/ 1_Confidence_1.000	AT5G09810	Hypothetical protein, peroxidase-like GDSL-like lipase	10	
NG-5590_Gland_cleanedcontig146154	Locus_258_Transcript_1/ 1_Confidence_1.000	AT3G52780	Purple acid phosphatase 20	12	
DM_TRA02_REP_contig79562	Locus_2276_Transcript_1/ 1_Confidence_1.000	AT5G48430	Aspartyl protease family protein-like	13	
DM_TRA02_contig126504	Locus_2818_Transcript_1/ 1_Confidence_1.000	AT1G68290	Actin	14	
DM_TRA02_contig120869	Locus_1790_Transcript_1/ 2_Confidence_1.000	AT3G50990	ENDO 2 (endonuclease 2)	17	
DM_TRA02_contig14293	Locus_1849_Transcript_1/ 1_Confidence_1.000	AT2G42840	Peroxidase superfamily protein PDF1 (protodermal factor 1)	17	
DM_TRA02_REP_contig72380	Locus_468_Transcript_1/ 1_Confidence_1.000	AT5G03240; AT3G	Ubiquitin extension protein	21	
DM_TRA02_REP_contig49581	Locus_1267_Transcript_1/ 1_Confidence_1.000	AT1G71695	Peroxidase superfamily protein	23	
DM_TRA02_contig137982	Locus_3385_Transcript_1/ 2_Confidence_1.000	XP_003536264	Peroxidase superfamily protein AAC3 (ADP/ATP carrier 3)	23	
DM_TRA02_contig14688	Locus_1267_Transcript_1/ 1_Confidence_1.000	AT4G28390	Peroxidase superfamily protein ATP synthase beta-subunit	28	
NG-5590_Gland_cleanedcontig79407	Locus_3385_Transcript_1/ 2_Confidence_1.000	AT5G22850	Aspartyl protease family protein (dionaeasin-2)	28	
				31	

TABLE II—continued

Identifier (454-transcript)	Identifier (Illumina-transcript)	Accession (A. thaliana)	Putative function	Average rank in both transcripts	
				Paper-based stimulation	Magnet-based stimulation
DM_TRA02_REP_contig50840	Locus_175_Transcript_1/ 1_Confidence_1.000	AT1G78300	G-box binding factor GF14 omega	34	34
	Locus_5247_Transcript_1/ 1_Confidence_1.000	AT3G12580	Heat shock protein 70	34	34
DM_TRA02_REP_contig60010		AT3G54420	ATEP3; chitinase	34	34
DM_TRA02_REP_contig56545		XP_003380422	superoxide dismutase [Trichinella spiralis]	35	35
DM_TRA02_contig7075		AT5G08680	ATP synthase beta-subunit	36	36
DM_TRA02_REP_contig48999		AT5G60390	elongation factor 1-alpha/EF-1-alpha	37	37
DM_TRA02_contig12608		AT1G68290	ENDO 2 (endonuclease 2)	38	38
DM_TRA02_contig1301		AT1G13440	Glyceraldehyde-3-phosphate dehydrogenase C2 (GAPC2)	39	39
DM_TRA02_contig16247	Locus_1944_Transcript_1/ 1_Confidence_1.000	AT4G37530	Peroxidase superfamily protein	40	40
DM_TRA02_contig13240		AT3G54420	ATEP3; chitinase	41	41
DM_TRA02_contig347	Locus_4642_Transcript_1/ 1_Confidence_1.000	AT5G67130	Phosphodiesterase superfamily protein	42	42
NG-5590_Gland_cleanedcontig105066		AT1G03220	Aspartyl protease family protein-like	42	42
DM_TRA02_REP_contig50509		AT5G02500	HSC70-1 (heat shock cognate protein 70-1)	44	44
DM_TRA02_contig28745			No BLAST hit with E-value < 1	45	45
DM_TRA02_REP_contig129322		AT5G41210	Glutathione transferase	48	48
DM_TRA02_contig16780		AT2G38460	Fructose-bisphosphate aldolase, putative	49	49
DM_TRA02_REP_contig48954		AT2G44490	Thioglucosidase	50	50
DM_TRA02_contig14440		AT5G17920	Methionine synthase	54	54
DM_TRA02_contig18374		AT2G03200	Eukaryotic aspartyl protease family protein (dionaeasin-1)	55	55

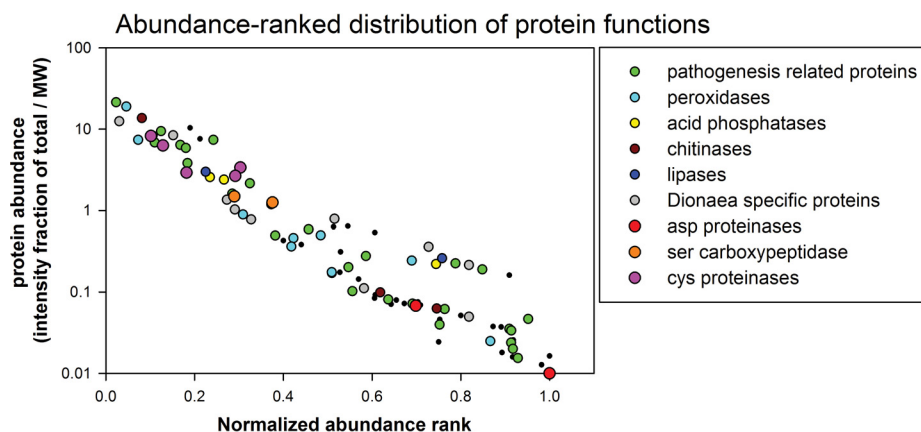


FIG. 2. The summed ion intensity fraction of the totals for the proteins identified in the two transcriptome versions plotted against the normalized abundance rank within the respective sample. Different colors indicate proteins of a similar function.

dures (Table II). However, the abundance ranking displayed differences between the two sampling procedures, emphasizing the importance of using complementary methods. The rankings based on MaxQuant and Mascot Distiller were generally in good agreement (supplemental Table S3). The 32 proteins identified from both transcriptome databases displayed significant identical overlaps over long, continuous stretches. Frequently, the shorter contig from one transcript was completely contained within another, longer transcript (supplemental Table S6). This finding clearly supports the value of the complementary approach utilized in this analysis of the Venus flytrap secretome.

In order to annotate the identified proteins based on function, the corresponding translated transcripts were homology searched against the well-annotated *Arabidopsis thaliana* proteome (supplemental Tables S4 and S5). Among the most abundant proteins in the Venus flytrap secretome were homologs of proteases, chitinases, osmotin-like protein, pathogenesis-related proteins, lipid transfer proteins, peroxidases, and beta-1,3-glucanase, which all belong to families of pathogenesis-related proteins (29). The presence of defense-related proteins has also been observed in the digestive fluid of *Nepenthes* (30), indicating that the digestive process in these two plants is functionally similar, although the plants belong to two different families, namely, *Droseraceae* and *Nepenthaceae*. Nine of the transcripts were homologous to different proteases, showing that the proteases are one of the two largest protein families in the secretome. This result correlates with the degrading function of the fluid. The sequence of one of the identified proteases was identical to the peptide sequence of a Venus flytrap digestive fluid cysteine protease from a previous study, except for one amino acid residue (16). In that particular study, the protease was termed “dionain.” Here, we adhered to this nomenclature and named the cysteine proteases dionain-1, dionain-2, dionain-3, and dionain-4. Dionain-1 is the protease that contains the previously sequenced peptides (Table II). Nine peroxidase homologs, including one of the top-ranking proteins from the filter-paper-based sampling procedure, were identified. These data indi-

cate that peroxidases have an important role in the digestive fluid. For each identified protein, we plotted the summed ion intensity fraction of the total against the normalized abundance rank in the two transcriptomes. The normalized abundance ranks were calculated as the abundance rank divided by the total number of proteins identified in each sample. When performing this ranking, it became apparent that proteins with antimicrobial/defense functions were among the most abundant proteins in the Venus flytrap secretion fluid (Fig. 2). Cysteine proteinases were consistently the most abundant proteases, followed by serine carboxypeptidases and aspartic proteases.

To strengthen our findings on the in-solution-based abundance ranking and composition analysis of the Venus flytrap digestive fluid, we conducted a complementary gel study (supplemental Fig. S1). Digestive fluid was collected from magnet-stimulated traps, and the proteins were separated on a silver-stained polyacrylamide gel prior to analysis via LC-MS/MS. The obtained spectra were queried against the *Illumina* transcriptome (supplemental Table S7). The majority of the proteins identified in the gel-based analysis were among the average top-10 ranked proteins present in the in-solution analysis of the magnet-based stimulation. Although there is a general relationship between the summed peptide intensities and the amount of protein present (27), outliers with very few tryptic peptides compatible with an MS analysis can also occur. This is likely to be the case for the relatively low ranking of the dionain-1 protein. This protein has been described previously as the major protein in the digestive fluid (16), and we identified this protein in four of the bands from the gel, which indicates the prominence of this protease. However, this protein was quantified by only one peptide, so its ranking is relatively low (supplemental Table S7).

The Proteolytic Enzymes of the Venus Flytrap Digestive Fluid—The protein sequences of four identified cysteine proteases were compared with those of other proteases using the MEROPS BLAST service (28). Dionains 1–3 and dionain-4 most resembled the cysteine proteases SPG31-like peptidase (31) and pseudotzain (32), respectively. All four proteases

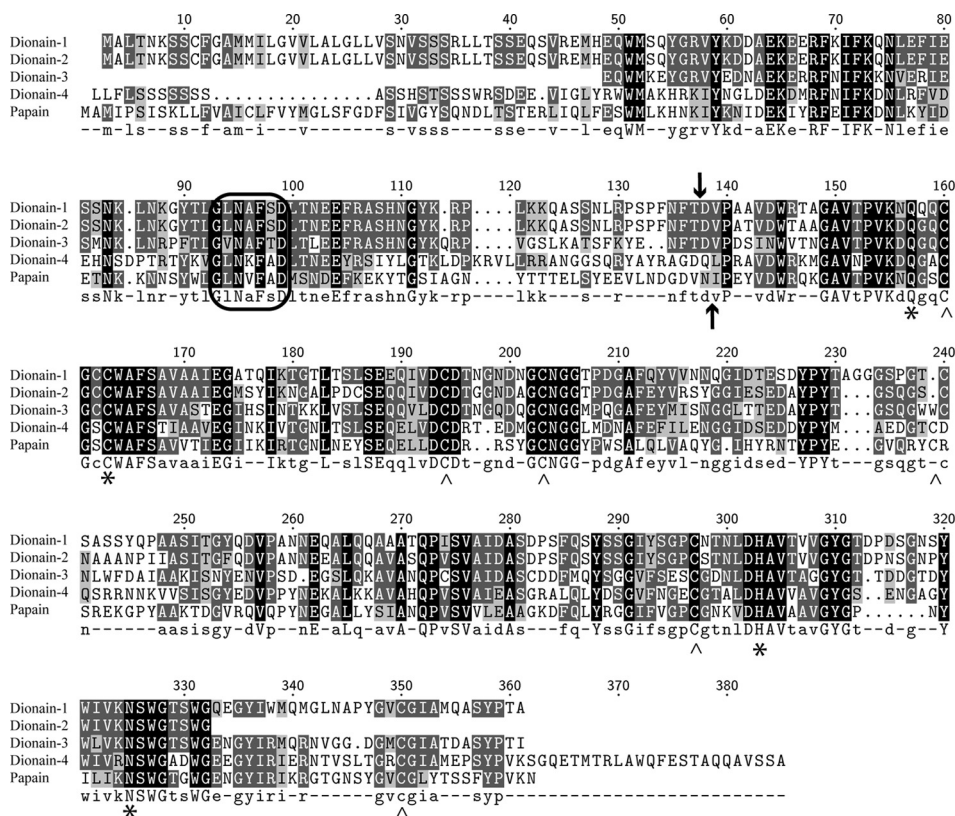


FIG. 3. The alignment of the open reading frames of the Venus flytrap cysteine proteases with papain. The encircled area represents a conserved motif that is essential for the conversion from zymogen to the mature protease in papain and cathepsin L. The upward-pointing arrow (↑) indicates the cleavage site between the activation peptide and the mature protease in papain, and the downward-pointing arrow (↓) indicates the cleavage site between the activation peptide and the mature protease in dionain-1. The asterisks (*) represent the active site residues in papain, and the carets (^) represent the cysteine residues involved in the disulfide bridges. The alignment strongly suggests that the active site residues and disulfide bridges are conserved between the five different plant cysteine proteases.

belong to the subfamily C1A, represented by the cysteine protease papain and to which the identified sequences were aligned (Fig. 3). The alignment illustrated that all of the reactive site residues and disulfide bridge-forming cysteines in papain were conserved in all of the dionains. The similarity to papain was also apparent because the pH optima of dionains are expected to be acidic, which is also the case for papain (33). In addition, the alignment showed that an evolutionarily conserved motif (Gly-Xxx-Asn-Xxx-Phe-Xxx-Asp), pivotal for the pH-dependent autoactivation of cysteine proteases, was present in the pro-peptide of the dionain activation mechanism. Indeed, SDS-PAGE of the digestive fluid proteins (collected in the absence of E-64) followed by the Edman degradation of dionain-1 (data not shown; also Ref. 16) revealed that activation occurred due to the proteolysis of a peptide bond within the same region observed for papain (Fig. 3).

The other large group of proteolytic enzymes in the secretome was the aspartic proteases. To characterize these proteases, the sequences were analyzed using BLAST against the MEROPS database, which demonstrated that

these proteases belong to subfamily A1B. This subfamily is represented by the nepenthesin from *Nepenthes gracilis* (36). The other large aspartic protease subfamily is A1A and is represented by pepsin, which is important for digestion processes in vertebrates. The main parts of the proteases in subfamilies A1A and A1B are most active at acidic pHs, but A1B differs from A1A in that it normally has six disulfide bridges, which are likely responsible for the remarkable stability of these proteins (37). Two of the identified aspartic proteases (contig 146154 and contig 105066 when using the 454 transcriptome naming) did not contain the active site residues found in the nepenthesins (Fig. 4). In addition, the cysteine patterns were different. These data indicate that although these proteases belong to the A1B subfamily, they are unable to display catalytic activities. An NCBI-BLAST search of these sequences indicated that the two proteins might be xylanase and endoglucanase inhibitor proteins, which are involved in plant defense (38). Taken together, two of the putative aspartic proteases are likely not involved in the degradation of prey proteins in the Venus flytrap.

In contrast, the other two Venus flytrap aspartic proteases contained the active site residues and nearly all of the disul-

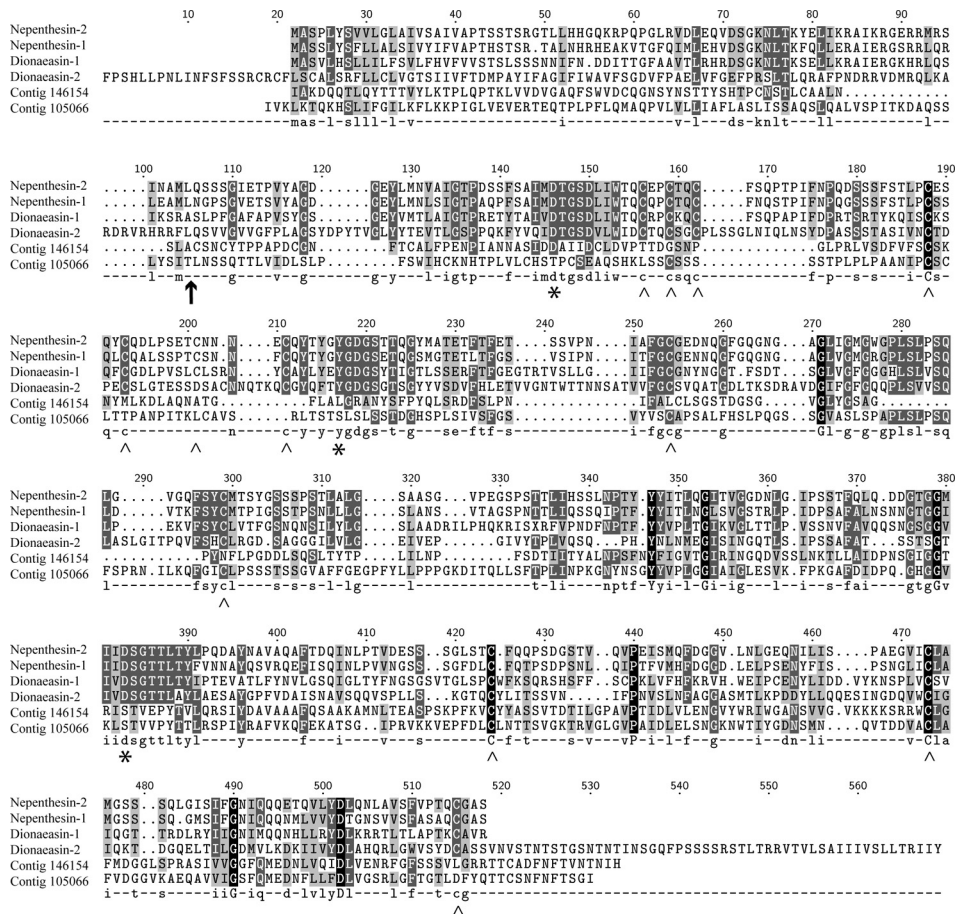


FIG. 4. The alignment of the Venus flytrap aspartate proteases with nepenthesin 1 and nepenthesin 2 identified from *Nepenthes gracilis*. The upward-pointing arrow (↑) indicates the cleavage site between the activation peptide and the mature nepenthesin proteases. The asterisks (*) represent the active site residues in the nepenthesins, and the carets (^) indicate the positions of the cysteine residues involved in the disulfide bridges in the nepenthesins. The alignment strongly suggests that two of the Venus flytrap aspartic proteases are catalytically active proteases (referred to as dionaecins), in contrast to the two other identified proteins (contigs 146154 and 105066), which are likely not catalytically active proteases.

vide bridge-forming cysteine residues at the same positions as in the nepenthesins. Consequently, we named these sequences dionaecin-1 (contig 18374) and dionaecin-2 (contig 79407), which is analogous to the nepenthesins from *Nepenthes*. These dionaecins are likely involved in prey digestion. However, these two proteases were less abundant in the digestive fluid than the cysteine proteases (Table II and Fig. 2), a finding also emphasized by the fact that dionaecin-1 was found in only one of the six LC-MS/MS analyses. These results suggest that aspartic proteases have a minor role in the degradation process. This is in contrast to *Nepenthes*, in which the nepenthesins are the most prominent proteolytic enzymes.

Regardless of the sampling procedure, the identified serine carboxypeptidase was relatively abundant (Table II), and it was identified using the less sensitive gel-based approach (supplemental Table S7). These results suggest that this protease has an important role in the digestion process. Sequence analyses revealed that it belongs to the S10 family of

serine proteases and to the plant serine carboxypeptidase III group (*MEROPS* ID S10.009) (39). The S10 family, represented by carboxypeptidase Y, is active only at acidic pHs, which makes it different from all of the other serine protease families (except for the S53 family). This activity at a low pH correlates with the finding of this protease in the acidic Venus flytrap digestive fluid.

DISCUSSION

Dionaea muscipula, the Venus flytrap plant, is not eaten by animals and is rarely infected by microbes due to its high content of defense metabolites and proteins (40). Instead, it actively traps, kills, and consumes animals. To gain insight into its digestive processes, we analyzed the composition of the fluid secreted by the plant. Most previous studies of the Venus flytrap's digestive fluid (13–15, 41) used an enzyme activity-based approach to characterize the composition of the fluid. In contrast to these indirect methods, we used a combination of transcriptomics and proteomics to identify the

major proteins present in the secreted fluid. Using the enzyme activity-based approach, protease, chitinase, peroxidase, phosphatase, and nuclease activities were detected (14, 15). With regard to protease activity, it has been suggested that the major protease in Venus flytrap digestive fluid is a cysteine protease and that carboxypeptidase activity is also present (14). With the present proteome study, we can explain these different enzymatic activities and correlate them with specific protein sequences.

Transcriptomics-facilitated Proteomics—A direct MS-based identification of the secreted proteins in Venus flytrap digestive fluid was complicated by the lack of the Venus flytrap genome. Recently, deep sequencing technologies have revolutionized the transcriptomics field (42). These methods are largely unbiased and high-throughput, and they provide a large dynamic range (43). To facilitate MS-based protein identifications and to obtain more sequence information, in contrast to a *de novo* MS approach, we used deep sequencing methods to produce a cDNA library of the transcribed mRNA sequences in stimulated Venus flytrap leaves (Fig. 1). The use of the assembled transcriptome as a database for protein identification was significantly more comprehensive and faster than *de novo* peptide sequencing. The rapid development of the “next-generation sequencing” field and the decreasing costs of this technology suggest that the approach applied here is generally applicable for proteome-based studies of organisms and systems for which genome sequence information is limited (44).

Secreted Proteins are Actively Synthesized in the Traps—The gel-based analysis of the secreted fluid confirmed that all of the major proteins (*i.e.* those visible on the silver-stained gel) in the digestive fluid were identified based on the transcriptome derived from the trap tissue. This analysis demonstrates that the cDNA sequences of the major secreted proteins are present in the transcriptome database. Indirectly, it shows that the mRNA coding for these proteins is present in the stimulated traps. Therefore, our results reveal that the Venus flytrap does not exclusively secrete proteins into the digestive fluid from preformed vesicles. Instead, the presence of mRNA indicates that the plant also synthesizes these proteins in the trap during the digestion process. These results are substantiated by the finding that only a limited amount of digestive fluid was present in the traps even after 24 h. If the proteins to be secreted had been present in storage vesicles and ready to be released, then we would have expected the digestive fluid at an earlier time point. These results are supported by previous findings showing that protein synthesis occurs during the secretory phase and that some of the synthesized protein is directly secreted (41).

Abundance Ranking of the Secreted Proteins—In total, 71% of the proteins identified upon magnet-based stimulation were also identified by filter-paper-based stimulation, demonstrating a large overlap between the two stimulation procedures. However, the abundance ranking displayed some dif-

ferences between the two procedures, at least when the integer ranks were compared. Because more proteins were identified using the filter-paper-based method, these rank numbers contained larger values than those from the magnet-based sampling. When the rankings were standardized for the number of identified proteins (Fig. 2), the abundances were more similar.

The low number of identified peptides for some of the proteins and the rather low abundance ranks likely can be explained by mispredicted nucleotides in some of the transcripts, which is consistent with previous findings demonstrating that contigs obtained from Illumina RNA-seq contain ~5% mispredicted nucleotides (45). Furthermore, the complete open reading frames were not sequenced for all of the transcripts, which can be partly explained by the low amounts of the respective mRNAs. In addition, the assembly programs used, Velvet and Mira, do not perform perfectly during redundancy reduction even at an error rate of 1% in the transcriptome (46).

The cysteine proteases were difficult to quantify and rank properly. These proteases contain a large activation peptide, and the arginine and lysine contents of the mature proteases are low; as a result, only a few tryptic peptides are applicable for MS analyses. These proteins also contain several glycosylation sites, which hamper MS-based identification. In addition, many of the peptides contain cysteine residues, and in our work these were more difficult to detect even though the proteins were alkylated. Thus, the ranking of *e.g.* dionain-1, the cysteine protease that was previously found to be a major component of the digestive fluid (16), was likely too low relative to its actual abundance. The high numbers of cysteine residues and putative disulfide bridges (Figs. 3 and 4) indicated that the identified proteins were compact and stable. Consequently, these proteins are likely to be relatively resistant to the promiscuous protease degradations taking place during digestion. Similar to other plant proteases (47), potential *N*-linked glycosylation sites indicate that the identified proteases could be glycosylated, stabilizing the proteins with respect to proteolytic degradation.

The Composition of the Digestive Environment Sheds Light on the Prey Digestion Mechanism—The low pH of the Venus flytrap digestive fluid is similar to that of other carnivorous plants (*e.g.* *Nepenthes*) and to the digestive fluid pHs among vertebrates. However, in vertebrates and *Nepenthes*, the proteolytically active enzymes are predominantly aspartic proteases (36, 48). In contrast, our findings suggest that cysteine proteases are the most abundant class of proteases in the digestive fluid of the Venus flytrap, followed by a serine carboxypeptidase and aspartic proteases. This composition and diversity of proteases has not been observed in other digestive fluids. The enzyme composition that resembles our findings the most is the intestinal protein digestion cascade employed by some invertebrates (49–51), which similarly includes aspartic proteases and cysteine proteases from the

same protease families (the pepsin family (A1) and the papain family (C1)) observed in the Venus flytrap. In general, cysteine proteases have a neutral pH optimum. However, adaptations to acidic pH optima have been observed among the lysosomal cathepsins, which are primarily involved in unspecific bulk protein degradation (52). The protease composition of the Venus flytrap's digestive fluid, with three classes of peptidases, is likely a potent digestion system, emphasizing the strong dependence of *Dionaea* on the nutrients supplied through prey capture and digestion (11). Particularly as the pH of the digestive fluid changes over time (7), the different enzymes might reach their maximum activities at different digestion stages after the prey is captured. As previously mentioned, the natural habitat of Venus flytrap plants is low-nutrient soils, and the plants depend on nutrients obtained by digesting trapped prey. These identified proteases are likely involved in the release of nitrogen from the prey proteins. In addition to proteases, a number of other hydrolytic enzymes are present in the digestive fluid, and the fact that nucleases, phosphatases, and phospholipases were identified indicates that phosphate is similarly obtained from the prey's nucleic acids, proteins, and cell membranes.

Three chitinases were also identified, including one of the proteins found to be most abundant in the digestive fluid regardless of the stimulation method. These chitinases would be expected to degrade the exoskeletons of captured insects or spiders and thereby facilitate enzymatic access to the inner part of the prey. Furthermore, chitinases are pathogenesis-related proteins that might prevent microbial growth on the trapped prey during the digestion process.

It has been suggested that prey proteins in the Venus flytrap are initially oxidized in order to facilitate their subsequent proteolysis (53), and it has been demonstrated that *Nepenthes gracilis* uses free radicals during the digestion process (54). Plumbagin, a low-molecular-weight compound present in Venus flytrap digestive fluid, likely facilitates this oxidation (40). The identified peroxidases from the present study are likely involved in these oxidative processes. Thus, our findings support the hypothesis that the oxidation of prey molecules facilitates the digestion mechanisms of the Venus flytrap.

The functions of the hydrolytic enzymes in the digestive fluid are intuitively easy to envision. These enzymes are likely directly involved in prey digestion. The functions of some of the other proteins present in the fluid are more challenging to elucidate, and a functional annotation based on the name of the best match in a homology search (Table II) does not necessarily shed light on the *in vivo* role of the protein. The roles of these proteins in the digestion mechanism remain to be investigated.

The Digestive Fluid Proteome Suggests a Shift from Defense-related Processes to Digestion-related Processes among the Carnivorous Plants—The only previously characterized digestive fluid proteome from a carnivorous plant was derived from *Nepenthes* (30). The depth of that *de novo* sequencing-based study was lower than in the present study;

however, aspartic proteases (nepenthesin I and II), a chitinase, a glucanase, a xylosidase, and a thaumatin-like protein were identified. These protein classes were, with the exception of the xylosidase, also identified in the present analysis of the Venus flytrap, indicating the conserved functions of the digestive fluid among carnivorous plant species. Similar to our results, the *Nepenthes* digestive proteins are also predominantly pathogenesis-related proteins. Higher plants express pathogenesis-related proteins as a response to an attack by pathogens, and consequently, many of these proteins possess hydrolytic activities that are potentially applicable to prey digestion in carnivorous plants. The identification of several defense-related proteins suggests that carnivorous plants have exploited the hydrolytic properties of these pathogenesis-related proteins (55). Many pathogenesis-related proteins are resistant to low pHs and to proteolytic degradation (29), making them functional in digestive fluids. During the evolution of carnivory in plants, there has likely been a shift from a pathogen-related response to a prey-related response and a shift from the hydrolysis and destruction of the pathogens to the hydrolysis and digestion of the prey. The defense-related proteins in digestive fluid likely still display antibacterial and antifungal effects, as in *e.g.* poplar extrafloral nectaries (22), in order to avoid pathogenic attacks during the digestion process.

CONCLUSION

The present characterization of Venus flytrap digestive fluid employed deep sequencing of the transcriptome followed by its assembly and subsequent use as a database during the proteomic analyses. This study demonstrates the use of high-throughput technologies in expanding molecular analyses to organisms for which the genome sequence is unknown. The Venus flytrap secretome reveals a unique diversity of hydrolytic enzymes, and the results shed light on the purpose and mechanisms of digestion. Furthermore, the *Dionaea* secretome contains a high proportion of pathogenesis-related proteins, suggesting that the capability of carnivorous plants to digest prey evolved from a plant defense system.

Acknowledgments—We thank Katharina Markmann (Aarhus, Denmark) and Tania A. Nielsen (Aarhus, Denmark) for help with RNA purification; Tom A. Mortensen (Aarhus, Denmark) and the nursery Lammehave (Denmark) for assistance and helpful suggestions regarding the cultivation of Venus flytrap plants; FASTERIS SA (Switzerland) for library preparation, Illumina sequencing, and Illumina transcriptome assembly; Kerstin Zander (Golm) for help in sample preparation for mass spectrometry; and Brigitte Neumann for excellent technical assistance (Würzburg).

* This work was supported by a grant from the Danish Research Council for Strategic Research to J.J.E. and an ERC Advanced Grant to R.H.

§ This article contains [supplemental material](#).

^a These authors contributed equally to this work.

** To whom correspondence should be addressed: Rainer Hedrich, E-mail: hedrich@botanik.uni-wuerzburg.de; and Jan Johannes Eng-hild, E-mail: jje@mb.au.dk.

REFERENCES

- Darwin, C. (1875) *Insectivorous Plants*, Murray, London
- Gibson, T. C., and Waller, D. M. (2009) Evolving Darwin's 'most wonderful' plant: ecological steps to a snap-trap. *New Phytol.* **183**, 575–587
- Forterre, Y., Skotheim, J. M., Dumais, J., and Mahadevan, L. (2005) How the Venus flytrap snaps. *Nature* **433**, 421–425
- Markin, V. S., Volkov, A. G., and Jovanov, E. (2008) Active movements in plants: mechanism of trap closure by *Dionaea muscipula* Ellis. *Plant Signal Behav.* **3**, 778–783
- Ueda, M., Tokunaga, T., Okada, M., Nakamura, Y., Takada, N., Suzuki, R., and Kondo, K. (2010) Trap-closing chemical factors of the Venus flytrap (*Dionaea muscipula* Ellis). *Chembiochem.* **11**, 2378–2383
- Williams, S. E., and Bennett, A. B. (1982) Leaf closure in the Venus flytrap: an acid growth response. *Science* **218**, 1120–1122
- Escalante-Perez, M., Krol, E., Stange, A., Geiger, D., Al-Rasheid, K. A., Hause, B., Neher, E., and Hedrich, R. (2011) A special pair of phytohormones controls excitability, slow closure, and external stomach formation in the Venus flytrap. *Proc. Natl. Acad. Sci. U.S.A.* **108**, 15492–15497
- Volkov, A. G., Carrell, H., Baldwin, A., and Markin, V. S. (2009) Electrical memory in Venus flytrap. *Bioelectrochemistry* **75**, 142–147
- Griggs, R. F. (1935) Victims of the Venus flytrap. *Science* **81**, 7–8
- Lichtner, F. T., and Williams, S. E. (1977) Prey capture and factors controlling trap narrowing in *Dionaea* (Droseraceae). *Am. J. Bot.* **64**, 881–886
- Schulze, W., Schulze, E. D., Schulze, I., and Oren, R. (2001) Quantification of insect nitrogen utilization by the Venus fly trap *Dionaea muscipula* catching prey with highly variable isotope signatures. *J. Exp. Bot.* **52**, 1041–1049
- Adamec, L. (1997) Mineral nutrition of carnivorous plants: a review. *Bot. Rev.* **63**, 273–299
- Takahashi, K., Matsumoto, K., Nishi, W., Muramatsu, M., and Kubota, K. (2009) Comparative studies on the acid proteinase activities in the digestive fluids of *NEPENTHES*, *CEPHALOTOUS*, *DIONAEA*, and *DROSEREA*. *Carnivorous Plant Newsletter* **38**, 75–82
- Robins, R. I., and Juniper, B. E. (1980) The secretory cycle of *Dionaea muscipula* Ellis. IV. The enzymology of the secretion. *New Phytol.* **86**, 401–412
- Scala, J., Iott, K., Schwab, D. W., and Semersky, F. E. (1969) Digestive secretion of *Dionaea muscipula* (Venus's-flytrap). *Plant Physiol.* **44**, 367–371
- Takahashi, K., Suzuki, T., Nishii, W., Kubota, K., Shibata, C., Isobe, T., and Dohmae, N. (2011) A cysteine endopeptidase ("dionain") is involved in the digestive fluid of *Dionaea muscipula* (Venus's fly-trap). *Biosci. Biotech. Bioch.* **75**, 346–348
- Hogslund, N., Radutoiu, S., Krusell, L., Voroshilova, V., Hannah, M. A., Goffard, N., Sanchez, D. H., Lippold, F., Ott, T., Sato, S., Tabata, S., Liboriussen, P., Lohmann, G. V., Schausser, L., Weiller, G. F., Urdvardi, M. K., and Stougaard, J. (2009) Dissection of symbiosis and organ development by integrated transcriptome analysis of lotus japonicus mutant and wild-type plants. *PLoS One* **4**, e6556
- Engelsberger, W. R., and Schulze, W. X. (2012) Nitrate and ammonium lead to distinct global dynamic phosphorylation patterns when resupplied to nitrogen-starved *Arabidopsis* seedlings. *Plant J.* **69**, 978–995
- Rasmussen, M. I., Refsgaard, J. C., Peng, L., Houen, G., and Hojrup, P. (2011) CrossWork: software-assisted identification of cross-linked peptides. *J. Proteomics* **74**, 1871–1883
- Cox, J., and Mann, M. (2008) MaxQuant enables high peptide identification rates, individualized p.p.b.-range mass accuracies and proteome-wide protein quantification. *Nat. Biotechnol.* **26**, 1367–1372
- Perkins, D. N., Pappin, D. J., Creasy, D. M., and Cottrell, J. S. (1999) Probability-based protein identification by searching sequence databases using mass spectrometry data. *Electrophoresis* **20**, 3551–3567
- Escalante-Perez, M., Jaborsky, M., Lautner, S., Fromm, J., Muller, T., Dittrich, M., Kunert, M., Boland, W., Hedrich, R., and Ache, P. (2012) Poplar extrafloral nectaries: two types, two strategies of indirect defenses against herbivores. *Plant Physiol.* **159**, 1176–1191
- Bury, A. F. (1981) Analysis of protein and peptide mixtures—evaluation of three sodium dodecyl sulfate-polyacrylamide gel-electrophoresis buffer systems. *J. Chromatogr.* **213**, 491–500
- Shevchenko, A., Tomas, H., Havlis, J., Olsen, J. V., and Mann, M. (2006) In-gel digestion for mass spectrometric characterization of proteins and proteomes. *Nat. Protoc.* **1**, 2856–2860
- Sanggaard, K. W., Karring, H., Valnickova, Z., Thogersen, I. B., and Engild, J. J. (2005) The TSG-6 and lalpal interaction promotes a transesterification cleaving the protein-glycosaminoglycan-protein (PGP) cross-link. *J. Biol. Chem.* **280**, 11936–11942
- Ishihama, Y., Oda, Y., Tabata, T., Sato, T., Nagasu, T., Rappsilber, J., and Mann, M. (2005) Exponentially Modified Protein Abundance Index (em-PAI) for estimation of absolute protein amount in proteomics by the number of sequenced peptides per protein. *Mol. Cell. Proteomics* **4**, 1265–1272
- Schwannhäusser, B., Busse, D., Li, N., Dittmar, G., Schuchhardt, J., Wolf, J., Chen, W., and Selbach, M. (2011) Global quantification of mammalian gene expression control. *Nature* **473**, 337–473
- Rawlings, N. D., Barrett, A. J., and Bateman, A. (2010) MEROPS: the peptidase database. *Nucleic Acids Res.* **38**, D227–D233
- van Loon, L. C., Rep, M., and Pieterse, C. M. (2006) Significance of inducible defense-related proteins in infected plants. *Annu. Rev. Phytopathol.* **44**, 135–162
- Hatano, N., and Hamada, T. (2008) Proteome analysis of pitcher fluid of the carnivorous plant *Nepenthes alata*. *J. Proteome Res.* **7**, 809–816
- Chen, G. H., Huang, L. T., Yap, M. N., Lee, R. H., Huang, Y. J., Cheng, M. C., and Chen, S. C. (2002) Molecular characterization of a senescence-associated gene encoding cysteine proteinase and its gene expression during leaf senescence in sweet potato. *Plant Cell Physiol.* **43**, 984–991
- Tranbarger, T. J., and Misra, S. (1996) Structure and expression of a developmentally regulated cDNA encoding a cysteine protease (pseudotzain) from Douglas fir. *Gene* **172**, 221–226
- Hoover, S. R., and Kokes, E. L. (1947) Effect of pH upon proteolysis by papain. *J. Biol. Chem.* **167**, 199–207
- Vernet, T., Berti, P. J., de Montigny, C., Musil, R., Tessier, D. C., Menard, R., Magny, M. C., Storer, A. C., and Thomas, D. Y. (1995) Processing of the papain precursor. The ionization state of a conserved amino acid motif within the Pro region participates in the regulation of intramolecular processing. *J. Biol. Chem.* **270**, 10838–10846
- Collins, P. R., Stack, C. M., O'Neill, S. M., Doyle, S., Ryan, T., Brennan, G. P., Mousley, A., Stewart, M., Maule, A. G., Dalton, J. P., and Donnelly, S. (2004) Cathepsin L1, the major protease involved in liver fluke (*Fasciola hepatica*) virulence: propeptide cleavage sites and autoactivation of the zymogen secreted from gastrodermal cells. *J. Biol. Chem.* **279**, 17038–17046
- Athauda, S. P. B., Matsumoto, K., Rajapakshe, S., Kuribayashi, M., Kojima, M., Kubomura-Yoshida, N., Iwamatsu, A., Shibata, C., Inoue, H., and Takahashi, K. (2004) Enzymic and structural characterization of nepenthesin, a unique member of a novel subfamily of aspartic proteinases. *Biochem. J.* **381**, 295–306; Erratum (2004) *Biochem. J.* **382**, 1039
- Takahashi, K., Athauda, S. P. B., Matsumoto, K., Rajapakshe, S., Kuribayashi, M., Kojima, M., Kubomura-Yoshida, N., Iwamatsu, A., Shibata, C., and Inoue, H. (2005) Nepenthesin, a unique member of a novel subfamily of aspartic proteinases: enzymatic and structural characteristics. *Curr. Protein Pept. Sci.* **6**, 513–525
- Sansen, S., De Ranter, C. J., Gebruers, K., Brijis, K., Courtin, C. M., Delcour, J. A., and Rabijns, A. (2004) Structural basis for inhibition of *Aspergillus niger* xylanase by triticum aestivum xylanase inhibitor-I. *J. Biol. Chem.* **279**, 36022–36028
- Drzymala, A., and Bielawski, W. (2009) Isolation and characterization of carboxypeptidase III from germinating triticale grains. *Acta Biochim. Biophys. Sin.* **41**, 69–78
- Tokunaga, T., Takada, N., and Ueda, M. (2004) Mechanism of antifeedant activity of plumbagin, a compound concerning the chemical defense in carnivorous plant. *Tetrahedron Lett.* **45**, 7115–7119
- Robins, R. J., and Juniper, B. E. (1980) The secretory cycle of *Dionaea muscipula* Ellis. II. Storage and synthesis of the secretory proteins. *New Phytol.* **86**, 297–311
- Shendure, J., and Ji, H. (2008) Next-generation DNA sequencing. *Nat. Biotechnol.* **26**, 1134–1145
- Wang, Z., Gerstein, M., and Snyder, M. (2009) RNA-Seq: a revolutionary tool for transcriptomics. *Nat. Rev. Genet.* **10**, 57–63
- Brautigam, A., Shrestha, R. P., Whitten, D., Wilkerson, C. G., Carr, K. M., Froehlich, J. E., and Weber, A. P. (2008) Low-coverage massively parallel pyrosequencing of cDNAs enables proteomics in non-model species: comparison of a species-specific database generated by pyrosequencing

- ing with databases from related species for proteome analysis of pea chloroplast envelopes. *J. Biotechnol.* **136**, 44–53
45. Wall, C. E., Cozza, S., Riquelme, C. A., McCombie, W. R., Heimiller, J. K., Marr, T. G., and Leinwand, L. A. (2011) Whole transcriptome analysis of the fasting and fed Burmese python heart: insights into extreme physiological cardiac adaptation. *Physiol. Genomics* **43**, 69–76
46. Bräutigam, A., Mullick, T., Schliesky, S., and Weber, A. P. (2011) Critical assessment of assembly strategies for non-model species mRNA-Seq data and application of next-generation sequencing to the comparison of C(3) and C(4) species. *J. Exp. Bot.* **62**, 3093–3102
47. Choi, K. H., and Laursen, R. A. (2000) Amino-acid sequence and glycan structures of cysteine proteases with proline specificity from ginger rhizome *Zingiber officinale*. *Eur. J. Biochem.* **267**, 1516–1526
48. Kageyama, T. (2002) Pepsinogens, progastricsins, and prochymosins: structure, function, evolution, and development. *Cell Mol. Life Sci.* **59**, 288–306
49. Williamson, A. L., Brindley, P. J., Knox, D. P., Hotez, P. J., and Loukas, A. (2003) Digestive proteases of blood-feeding nematodes. *Trends Parasitol.* **19**, 417–423
50. Delcroix, M., Sajid, M., Caffrey, C. R., Lim, K. C., Dvorak, J., Hsieh, I., Bahgat, M., Dissous, C., and McKerrow, J. H. (2006) A multienzyme network functions in intestinal protein digestion by a platyhelminth parasite. *J. Biol. Chem.* **281**, 39316–39329
51. Knox, D. (2011) Proteases in blood-feeding nematodes and their potential as vaccine candidates. *Adv. Exp. Med. Biol.* **712**, 155–176
52. Barrett, A. J. (1992) Cellular proteolysis. An overview. *Ann. N.Y. Acad. Sci.* **674**, 1–15
53. Galek, H., Osswald, W. F., and Elstner, E. F. (1990) Oxidative protein modification as predigestive mechanism of the carnivorous plant *Dionaea muscipula*: an hypothesis based on in vitro experiments. *Free Radic. Biol. Med.* **9**, 427–434
54. Chia, T. F., Aung, H. H., Osipov, A. N., Goh, N. K., and Chia, L. S. (2004) Carnivorous pitcher plant uses free radicals in the digestion of prey. *Redox Rep.* **9**, 255–261
55. Mithofer, A. (2011) Carnivorous pitcher plants: insights in an old topic. *Phytochemistry* **72**, 1678–1682
56. Schulz, M. H., Zerbino, D. R., Vingron, M., and Birney, E. (2012) Oases: robust de novo RNA-seq assembly across the dynamic range of expression levels. *Bioinformatics* DOI: 10.1093/bioinformatics/bts094
57. Dyrlund, T. F., Poulsen, E. T., Scavenius, C., Sanggaard, K. W., and Enghild, J. J. (2012) MS Data Miner: a web-based software tool to analyze, compare and share mass spectrometry protein identifications. *Proteomics*, in press, DOI: 10.1002/pmic.201200109